

## Surface Tension of Symmetric Star Polymer Melts

Zhenyu Qian,<sup>†</sup> Venkatachala S. Minnikanti,<sup>†</sup> Bryan B. Sauer,<sup>‡</sup> Gregory T. Dee,<sup>‡</sup> and Lynden A. Archer<sup>\*,†</sup>*School of Chemical and Biomolecular Engineering, Cornell University, Ithaca, New York 14853, and Central Research and Development, Experiment Station, DuPont, Wilmington, Delaware 19880**Received October 23, 2007; Revised Manuscript Received April 17, 2008*

**ABSTRACT:** To evaluate the effect of polymer architecture on surface tension, glass transition, and other thermodynamic properties, we synthesized a series of 4-arm and 11-arm symmetric star polystyrenes. Surface tension was measured as a function of molecular weight of the stars and temperature in the melt using a modified Wilhelmy plate technique. We find that architectural effects play a significant role in determining the molecular weight dependence of polymer melt surface tension. A variable density lattice model that considers effects of entropic attraction of polymer chain ends to surfaces, compressibility and density gradients in the region near the surface is used to determine the origin of this observation. This analysis is complemented with surface tension calculations using more classical thermodynamic models that consider only bulk property changes with polymer architecture and molecular weight. Bulk thermodynamic properties for selected stars were derived from pressure–volume–temperature (PVT) measurements. These data are used to calculate the cohesive energy density (CED). This was then used to determine surface tension of the stars using a recently developed theory. Possible effects of the chemical differences of the *sec*-butyl terminal groups versus the backbone segments are also discussed in terms of bulk property modification and surface segregation of end groups.

## Introduction

The surface tension of a molecular fluid is its excess free energy per unit area of surface.<sup>1</sup> For small-molecule liquids, the excess energy results from missing neighbors at the surface, and the surface tension is completely specified by the energetic interactions between molecules in the bulk.<sup>1</sup> The surface tension of a polymer is generally higher than that of a liquid of its unconnected constituent monomers both because the number of accessible molecular conformations is lower at the surface,<sup>2</sup> and the bulk density of the polymer molecule is higher.<sup>3,4</sup> There are two principle approaches to the theory of polymer melt surface tension. The first focuses on the limit of high molecular weight ( $M_n$ ) and uses lattice models to predict the entropic and enthalpic contributions in the limit of large  $M_n$ . For a linear polymer in the limit of high  $M_n$ , this “entropic” contribution to the excess surface energy varies as  $B - CM_n^{-\alpha}$ , where  $\alpha$  is a positive number of order unity,<sup>2,5–11</sup>  $B$  is the “infinite molecular weight” contribution to the surface tension, and the parameter  $C$  quantifies the decrease in the infinite molecular weight conformational entropy contribution for finite polymer molecular weights. At large  $M_n$ , the generally larger “local” enthalpic contribution to the surface tension is also expected to be of the form,  $D - EM_n^{-1}$ . This form simply assumes that the local enthalpic contribution follows a reciprocal dependence on  $M_n$  analogous to other bulk thermodynamic properties (the end group effect).<sup>4</sup> Equation of state models can be used to both describe this molecular weight dependence,<sup>4</sup> and to estimate the coefficients  $D$  and  $E$ .

In the high molecular-weight limit, it was proven experimentally several years ago that the surface tension varies as  $M_n^{-1}$ ,<sup>12</sup> while it has been known for a much longer time that for very low  $M_n$  that the dependence is weaker,  $\gamma: \sim M_n^{-2/3}$ .<sup>12,13</sup> As almost all other bulk properties vary as  $M_n^{-1}$ ,<sup>4,14</sup> this latter observation has sparked much interest.<sup>13</sup>

There are many possible contributions of polymer chain ends to the molecular weight dependence of surface tension. First,

chemical heterogeneity of end segments, compared with the middle segments, can produce enthalpic attraction of chains to the surface. It can also modify the bulk thermodynamic properties, including density, of the entire material, which influences the surface tension. Second, chain ends have extra degrees of freedom inaccessible to other segments of a polymer chain.<sup>4</sup> For large molecules, this leads to configurational entropy differences within the chain, wherein the whole polymer chain experiences a greater penalty than the ends for residence at a surface.<sup>2</sup> In this work, we perform variable density SCF lattice simulations and apply classical thermodynamic models to understand the roles played by both effects on the surface tension of symmetric star and linear polystyrenes. A straightforward comparison between experimental data and ideal theoretical calculations allows the relative importance of these effects to be evaluated.

The literature of how surface/bulk properties of branched macromolecules affects their surface activity is sparse.<sup>15–23</sup> Detailed experiments by Elman et al.<sup>15</sup> and Jalbert et al.<sup>16,17</sup> have explored surface and interface segregation of polymers containing end groups that are neutral, attractive and repulsive to surfaces. Elman et al.<sup>15</sup> reported experimental evidence for surface enrichment/depletion of the corresponding end groups from neutron reflection studies of end functionalized polystyrenes. End group effects on surface tension have proven very difficult to confirm experimentally. Surface excess profiles of deuterated and hydrogenated PS blends have shown that the surface tension may not be substantially modified by the presence or absence of a *sec*-butyl chain end.<sup>18</sup>

Lee and Foster<sup>19,20</sup> anionically synthesized regularly branched molecules (polybutadiene and polystyrene), and studied thermodynamic properties, such as glass transition temperature, thermodynamic bulk interaction parameters, and phase diagrams of these branched molecules blended with their linear counterparts. Walton, Irvine, Mayes et al.<sup>21–23</sup> performed self-consistent mean-field lattice simulation blends of branched and linear polymers, and also experimentally studied the surface functionalization of a polylactide bioscaffold by utilization of a comblike additives. Both simulation and experimental results indicate surface segregation of branched architectures.

\* Corresponding author.

<sup>†</sup> School of Chemical and Biomolecular Engineering, Cornell University.

<sup>‡</sup> Central Research and Development, Experiment Station, DuPont.

## Theoretical Background

Compressible lattice theories that consider the effects of polymer chain entropy, finite compressibility, and density gradients on surface properties (e.g., surface tension and surface excess composition of a more surface active species in a blend), have recently been developed for polymer systems of widely varying architectures.<sup>11,23</sup> Similar analyses based on incompressible lattice models underpredict these properties, indicating that the melt compressibility is an important determinant of the surface behavior. Linear response theory in the limit of high  $M_n$  has been shown to provide a good method for approximating surface properties obtained either using incompressible or compressible lattice models.<sup>11,24</sup> This theory is advantageous for analyzing surface tension data because it yields a simple, analytical formula for the surface tension  $\gamma_M$  of an arbitrarily branched polymer with a functional form similar to those described above.<sup>9–11</sup>

$$\gamma_M \cong \gamma_{\infty} + \frac{\rho_b RT (n_e U^e + n_j U_{ne}^j)}{M_n} \quad (1)$$

Here,  $\gamma_{\infty}$  is the surface tension of a theoretical infinite  $M_n$  polymer, which includes a contribution from the conformational constraints experienced by polymers in the limit of infinite molecular weight, and  $n_e$  and  $n_j$  are, respectively, the number of ends and branch points.  $U^e$  and  $U_{ne}^j$  can be interpreted, respectively, as the “effective” attraction and repulsion of the ends and branch points to the surface. Considering chain ends to be chemically identical to the midsections, this model predicts that polymer chain ends are attracted toward the surface and the branch point is repelled away from it<sup>9,10</sup> making  $U^e$  negative and  $U_{ne}^j$  positive. Thus, even for the simplest branched polymer structure (the symmetric star), for which  $n_j = 1$ , this equation predicts that the surface tension can be manipulated by changing the number of star arms. Furthermore, because  $U^e$  can also be a function of polymer chain-end chemistry, the effect can be amplified by these additional energetic components, as already illustrated for linear<sup>16,25</sup> and hyperbranched polymers<sup>26</sup> by suitable end functionalization of chain ends. In extreme cases of end-group modified linear polymers, Jalbert et al.<sup>16</sup> and McLain, et al.,<sup>25</sup> have in fact shown that such energetic contributions can provide a substantial driving force for a surface excess of chain ends.

It is well-known that the larger degree of freedom associated with chain ends can also have a dramatic effect on the way bulk properties, such as density, glass transition, and cohesive energy density (CED), vary with polymer molecular weight.<sup>14</sup> Dee and Sauer have shown that PVT data for many polymers and oligomers can be used to calculate their surface tension.<sup>4,27–29</sup> This methodology ignores all aspects of chain architecture, or even chain connectivity, but is found to account very well for bulk thermodynamic property differences from changes in chemical structure and especially changes in  $M_n$ . These models<sup>27–29</sup> can also partially account for the configurational entropy penalty of having high  $M_n$  chains at sharp interfaces.<sup>2</sup>

An equation of state (EOS) provides a simple means of capturing the thermodynamic information contained in measured PVT data.<sup>4,30</sup> The Flory, Orwoll, and Vrij (FOV) equation has been extensively used to represent thermodynamic data for polymer melts.<sup>31</sup> It can be adapted to provide an analytical expression for the surface tension of a liquid,<sup>32</sup>

$$\gamma^* = \gamma/\gamma^* = \left\{ -\frac{m}{\tilde{V}} - T \ln \left[ \frac{b \tilde{V}^{1/3}}{\tilde{V}^{1/3} - 1} \right] \right\} / \tilde{V}^{2/3} \quad (2)$$

Here  $\gamma^* = (0.11kP^*T^*)^{1/3}$ ,  $k$  is Boltzmann’s constant, where  $\tilde{V} = v_{sp}/v_{sp}^*$  is the reduced specific volume, and  $P^*$ ,  $T^*$ , and

$v_{sp}^*$  are the critical pressure, temperature, and specific volume. These parameters are obtained by fitting the FOV EOS to thermodynamic data. Equation 2 evidently has both an enthalpic and an entropic component. The relative magnitude of the two can be captured empirically by the values of the parameters  $m$  and  $b$ .<sup>27,28,32</sup> For many polymers, this methodology yields estimates for the surface tension that are in good agreement with experimentally determined values.<sup>27,29</sup>

## Experimental Section

Benzene (Aldrich, >99%) and styrene were respectively purified using *n*-butyllithium and dibutylmagnesium. Living polystyrene chains with a range of molecular weights were synthesized using standard anionic techniques and *sec*-butyllithium initiator. The polymerization reaction was initiated on a vacuum line and transferred to a MBraun glovebox, where the polymerization was allowed to proceed for 24 h under protection of nitrogen gas “boil off” from a liquid nitrogen source. To produce symmetric star polymers, the living poly(styryl)lithium chains were mixed in purified benzene with two multifunctional chlorosilane linking agents, bis(methyldichlorosilyl)butane (Gelest, >95%), to produce 4-arm stars, and 1,2,3,4,5,6-hexakis[(2-methyldichlorosilyl)ethyl]benzene, to produce 11-arm stars. A large excess of poly(styryl)lithium living chains ([Si–Cl/PS–Li]) was added to the selected linking agent to ensure high linking efficiency. The reactants were continuously stirred for several days to ensure that the linking reaction goes to completion. Excess living chains were terminated by degassed isopropanol. Salts created in the termination and linking steps were removed in a water wash performed in a separating funnel. Highly purified star polymers were obtained by fractionation in a good solvent–poor solvent (toluene–methanol) mixture.

Molecular weights of the resultant star polystyrenes and their linear precursors were characterized using matrix-assisted laser desorption ionization time-of-flight (MALDI–TOF) mass spectrometry (MacroMass). Dithranol and trifluoroacetate were used as the matrix and cationizing agent, respectively. MALDI–TOF measurements were complemented by size exclusion chromatography (SEC), performed using a Viscotek SEC comprised of four mixed bed columns and equipped with a laser light scattering detector (TDA302). Because of their small size, MALDI–TOF provides a more accurate means of characterizing the precursor molecular weight. Table 1 shows that for the 4-arm star polystyrene series, the experimentally determined molecular functionality is very close to the theoretical value, 4, for the linker used, irrespective of the arm molecular weight. In the case of the “11-arm” series, MALDI–TOF indicates functionalities close to 11, which is slightly lower than the theoretical maximum of 12 for the specific linker used. These differences are expected for high arm functionalities such as those attempted here, and can arise from multiple sources, including imperfection of the 1,2,3,4,5,6-hexakis[(2-methyldichlorosilyl)ethyl]benzene linker itself and the steric hindrance around the branch point. Molecular weights of the linear precursors of the 4-arm and 11-arm stars, the actual star functionalities, polydispersities, and glass transition temperatures are given in Table 1.

The “micro”-Wilhelmy wetting method<sup>12</sup> was used for molten polymer surface tension measurements. In this method the standard Wilhelmy plate<sup>13</sup> is replaced by a small-diameter clean glass fiber. A large increase of the viscous relaxation rate of the wetting meniscus due to the small wetting probe size provides substantially increased accuracy.<sup>4,12,33</sup> Only about 0.1 g of sample is required for the measurements. For relatively nonpolar high surface energy polymers like high- $M_w$  PS, wetting can become marginal at temperatures below 200 °C.<sup>34</sup> This finite contact angle can affect the liquid or melt surface tension measured by Wilhelmy plate or fiber techniques, even with a “clean” glass surface.<sup>35</sup> The surface tension values for many of the PS stars studied and lower  $M_w$  linear chains are sufficiently low that incomplete wetting or nonzero contact angles above 160 °C only have a negligible effect on the measurements. This effect arises from the fact that the polymer surface tension decreases as temperature rises, while the glass

Table 1. Polymer Characterization

no. of arms	PS sample	$M_n$ of arm <sup>a</sup>	$M_n$ of star PS <sup>a</sup>	PDI of star PS <sup>b</sup>	functionality <sup>c</sup>	$T_g$ (°C)
4	R25	470	2000	1.03	4	45
	R26	1150	4800	1.03	4.1	69
	R27	1500	6300	1.02	4.1	79
	R28	1750	7400	1.03	4.2	84
	R29	3200	12600	1.01	3.9	90.5
	R30	4000	16.8	1.03	4	93.8
11	R33	510	5900	1.03	10.6	64
	R34	660	7500	1.03	10.6	69
	R35	760	8800	1.03	10.9	73.5
	R36	1400	15800	1.04	10.9	81.5
	R37	2680	29000	1.04	10.6	92
	R38	5400	59000 <sup>b</sup>	1.03	10.8	100.5

<sup>a</sup> Measured by MALDI-TOF. <sup>b</sup> Measured by SEC. <sup>c</sup> Estimated from  $(M_{n,star} - M_{n,core})/M_{n,arm}$ .

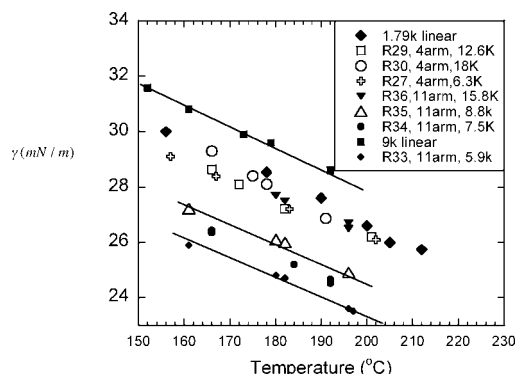


Figure 1. Temperature dependent surface tension for representative linear, 4-arm star, and 11-arm star PS with different molecular weights.

surface free energy remains approximately constant due to its low thermal expansion coefficient.<sup>35</sup> Reliable surface tension measurements for nonpolar polymers such as PS, also require that adsorbed water on the glass surface is minimized.<sup>35</sup>

A Gnomix dilatometer was used for the *PVT* measurements of linear PS controls as described previously.<sup>30</sup> Because of the large sample volume required for these measurements, they were limited to a single representative 4-arm and one 11-arm star. Differential scanning calorimetry (DSC) (TA Instruments 2920, New Castle, DE) was used to determine the midpoint glass transition temperature ( $T_g$ ) of all materials used in the study.

## Results and Discussion

The surface tension for all polymers studied was measured as a function of temperature. Figure 1 provides temperature dependent surface tension data for representative linear and star PS molecules with molecular weights,  $M_n$ , in the range 1.8K to 20K. It is apparent from the figure that the slopes for all polymers are quite similar. This observation implies that changes in thermal expansion and other related bulk properties are unaffected by polymer molecular weight and architecture in the range studied. Comparison of the surface tension data at fixed temperature, however, reveals large changes with molecular weight and architecture over this same range. Figure 2, for example, illustrates both the effect of polymer molecular weight and architecture on  $\gamma$  at a temperature of 160 °C. The values of  $\gamma$  for linear, 4-arm, and 11-arm symmetric star polystyrenes all manifest approximately linear dependences on  $1/M_n$ , with architecture-dependent slopes. The results in the figure indicate that polystyrenes with unusually low surface tension can be accessed at modest molecular weights simply by increasing the number of arms in the stars. This effect has never been seen before in such a series, especially at the higher branch numbers.

A straight-line fit of the experimental surface-tension values in Figure 2 yields an architecture-independent intercept  $\gamma_{\infty}$ , and

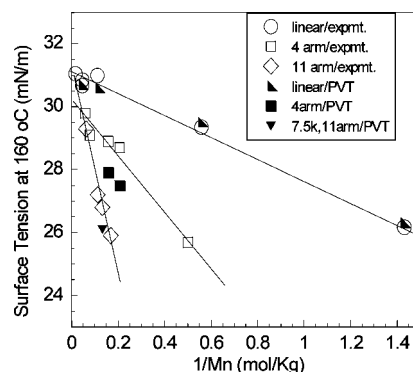


Figure 2. Surface tension  $\gamma_M$  of linear and star polymers as function of inverse molecular weight  $M_n^{-1}$  at 160 °C. Circles are linear PS, squares 4-arm star PS, and diamonds 11-arm star PS. The filled symbols are the predictions based on the *PVT* analysis, discussed later, for the respective systems.

Table 2. Initial Slope of Surface Tension vs Inverse Molecular Weight<sup>a</sup>

polymer architecture	$\rho_b RT(n_e U^e + U_{ne}^j)$ (mJ·Kg/m <sup>2</sup> ·mol)	
	model value	experimental value
linear	-4.6	-3
4-arm star	-7.1	-10
11-armstar	-20.2	-28

<sup>a</sup> With values of  $U^e = -0.651$  nm,  $U_{ne}^j = 0.607$  nm, and  $U_{11}^j = 1.503$  nm, estimated through entropic consideration using self consistent field theory of a polymer on a variable density lattice model.<sup>11</sup>

a slope of  $\rho_b RT(n_e U^e + U_{ne}^j)$ . These fits yield  $\gamma_{\infty} \sim 30.8$  mN/m, consistent with that extracted from published data for the linear controls.<sup>4</sup> Table 2 summarizes the slopes, and the theoretical predictions will be discussed below. The major factor governing  $\gamma$  is evidently the presence of chain ends. This is seen qualitatively in Figure 3 where the data are observed to converge to an approximate universal curve when normalized to account in some way for the ends. More specifically, the  $M_n$  of the arms appears to empirically scale the data but only if the linear molecule is assumed to have one end; i.e., the  $M_n$  for the "arm" is the  $M_n$  of the entire chain.

It is possible to estimate the contribution of the attraction of ends and repulsion of branch points to the surface tension of symmetric star polymers from self-consistent field theory (SCF) simulations of a polymer on a lattice in the framework of Scheutjens and Fleer.<sup>36</sup> The technique to estimate these entropic potentials is described elsewhere.<sup>9,10</sup> If a lattice polymer is considered to be completely incompressible, the value of the entropic attraction of the ends  $U^e$  is found to be  $-0.0975$  in lattice spacing units.<sup>10</sup> On a lattice, a polymer is typically considered to make a random walk on a length scale of a Kuhn length.<sup>36</sup> Hence taking a lattice spacing as one Kuhn unit which for polystyrene is 1.8nm,<sup>37</sup> one obtains a value for  $U^e$  to be



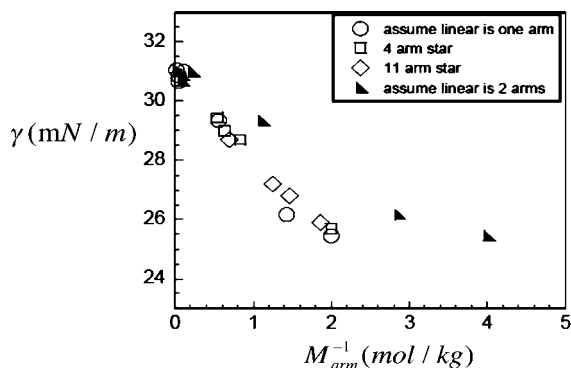


**Figure 3.** Surface tension  $\gamma_M$  of linear and star polymers at 160 °C as function of corrected inverse molecular weight. The term  $M_{\text{arm}}^{-1}$  is used to correct for the number of chain ends. Open circles are linear PS assumed to have 1 arm, open squares are 4-arm star PS, and open diamonds represent 11-arm star PS.

−0.1755 nm. As is the case here, Kumar and Jones<sup>38,39</sup> have shown that considering a polymer to be incompressible significantly underestimates the derivative of surface tension with inverse molecular weight  $d\gamma/(d1/M)|_{M \rightarrow \infty}$ . Wu and Fredrickson considered the effect of finite compressibility on the linear response theory, but nonetheless compute the surface tension only in the incompressible limit.<sup>8</sup> Walton and Mayes<sup>23</sup> also performed self-consistent mean-field calculations to study the effect of chain architecture on surface segregation. These authors found that the finite compressibility of polymer chains influence  $\gamma$  through its effect on density gradients at the surface. Minnikanti and Archer<sup>10,11</sup> showed that compressibility effects significantly increase the effective chain end attraction to a surface. Using a variable density lattice model that considers the effects of finite compressibility and density gradients,<sup>10</sup>  $U^e$  for a polystyrene like lattice polymer at 160 °C was estimated to be −0.651 nm, which is substantially larger than the value −0.1755 nm deduced for the incompressible model. In a similar fashion the entropic repulsion of the joint point of a branched molecule with  $n_c$  branches can be estimated.<sup>10</sup> These values can be used to estimate the variable  $\rho_b RT(n_c U^e + n_j U_{\text{ne}}^j)$  for the linear and symmetric star polymers, the results are compared with their experimentally determined counterparts in Table 2. Here  $\rho_b$  is taken to be the mass density of an infinite molecular weight polystyrene at 160 °C and is determined using experimental data fit to the Sanchez and Lacombe (SL) equation of state<sup>40</sup> to be 989 kg/m<sup>3</sup>, and  $U^e$  is computed in the variable density lattice model. It is evident from the table that the theoretical and experimentally determined slopes are in reasonably good agreement for the linear, 4-arm, and 11-arm stars. Considering the lack of precision of the experimental data, and the qualitative nature of the variable density contributions effectively extracted from the SL equation of state and used in the prediction of  $U^e$  and  $U_{\text{ne}}^j$ ,<sup>10</sup> the theoretical prediction could be considered as quite good.

The chemical difference between the chain ends, linker, and backbone styrene segments can make contributions to  $U^e$  and  $U_{\text{ne}}^j$ . Additionally, eq 1 is strictly only correct in the limit when the radius of gyration of the polymer is large compared to the Kuhn step length, which is not true for some of the polymers studied. For some of our samples, each arm is only about one Kuhn segment, so some deviation of the model prediction at low molecular weight is expected. However, for each architecture studied there are several samples of high-enough molar mass that lattice simulations can be regarded as predictive. Finally, the variable density lattice SCF calculations themselves introduce several well-documented errors.<sup>36</sup> Considering all of these potential sources of error, the good agreement between the calculated and experimental slopes seen in Table 2 imply

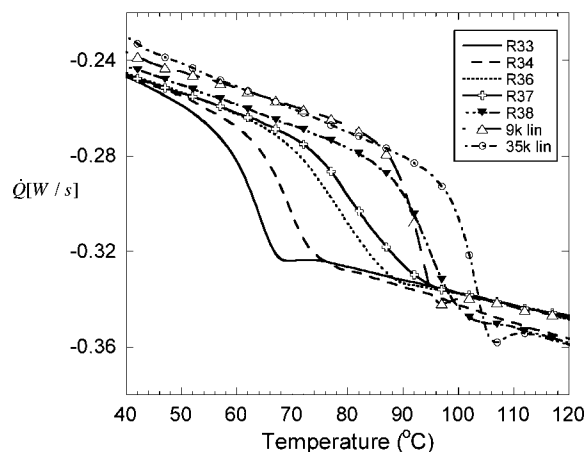


**Figure 4.** Differential scanning calorimetry (DSC) curves showing the glass transition temperature region for 11-arm star PS samples of different molecular weights and for 2 linear PS control samples.  $\dot{Q}$  is the heat flow rate.

that the variable density lattice calculations capture many of the important physics governing the surface tension of star molecules. Specifically, the comparisons show that the effect of polymer “architecture” on variable density lattice analysis of surface tension can by itself account for much of molecular weight on the surface tension of symmetric star polystyrenes.

One could go a step further in this analysis to obtain a rough estimate of the specific contribution made by chain end chemical heterogeneity to the surface tension. Specifically, the end attraction per arm,  $U^e$ , can be separated into an “architecture”  $U_a^e$  contribution and a chemical  $U_c^e$  contribution ( $U^e = U_a^e + U_c^e$ ). The latter contribution reflects chemical differences between chain ends and midsections. If all other sources of discrepancy between the variable density lattice SCF calculated slopes and the measured ones (Table 2) are ignored,  $U_c^e$  can be readily computed for the 4-arm and 11-arm stars. This calculation yields  $U_c^e \approx -0.852$  nm for the 11-arm stars and  $U_c^e \approx -0.854$  nm for the 4-arm stars. The similarity of the two values is consistent with what one would expect for stars, such as the ones used in the study, where the chain end chemistry is the same (i.e., *sec*-butyl). The values of  $U_c^e$  also show that the end-group chemistry has a significant effect on the surface tension of the stars (its contribution to  $U^e$  is comparable to that provided by the purely entropic attraction of chain ends). Its overall effect on the experimentally deduced values of  $d\gamma/(d1/M)|_{M \rightarrow \infty}$  is nonetheless modest, at most 35% for the 4-arm and 11-arm stars.

As pointed out earlier, chain-end attraction to a surface is not the only mechanism through which molecular architecture can influence surface tension. Specifically, architectural changes to bulk properties, such as glass transition temperature and density can play an important role. Figure 4 provides DSC data for a wide range of 11-arm stars, and two linear controls. The glass transition for the stars are generally slightly broader than for the linear controls. R37 is one of the highest molecular weight polymers ( $M_n = 29\,000$  kg/mol), but is comprised of low molecular weight arms ( $M_n = 2680$  kg/mol). The arms on all the others stars are substantially shorter, and may contribute to the breadth of  $T_g$  because the centers of the molecules are rigid. Glass transition temperatures for the linear and star polymers deduced from the DSC data are presented in Figure 5 as a function of polymer molecular weight. It is apparent from the figure that  $T_g$  becomes progressively lower with increasing number of branches at a given total polymer  $M_n$ . These results are roughly consistent with changes anticipated from the larger degrees of freedom associated with chain ends.<sup>14,41</sup> It is also

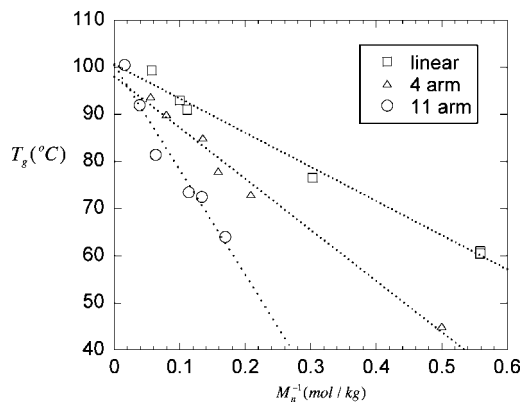


**Figure 5.** Glass transition temperature ( $T_g$ ) of linear and star polymers as function of inverse molecular weight  $M_n^{-1}$ . Squares are linear PS, triangles 4-arm star PS, and circles 11-arm star PS.

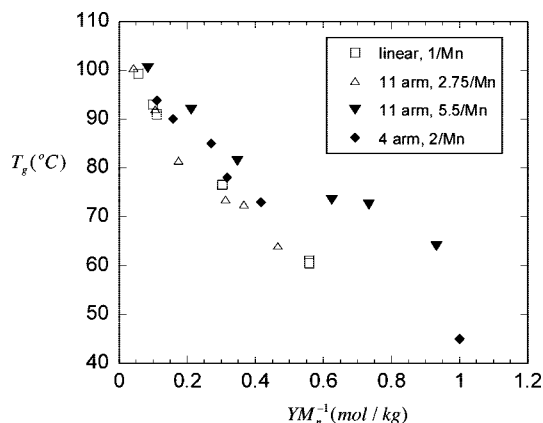


**Figure 6.** Glass transition temperature ( $T_g$ ) of linear and star polymer as function of inverse molecular weight of the longest chain segment. Squares are linear PS, diamonds 4-arm star PS, and triangles 11-arm star PS.

possible that the *sec*-butyl end group has some contribution. The extrapolated  $T_g$  in the limit of infinite  $M_n$  is also seen to be approximately the same for the stars and linear materials, also in agreement with previous studies.<sup>42,43</sup> Normalization of the data to the length of the longest chain segment (i.e., number of arms/ $[2M_n]$ ), overcorrects the  $T_g$  data for the 11-arm (i.e.,  $5.5/M_n$ ) (see Figure 6). This observation indicates that the effect of the increased number of chain ends on the glass transition is partially counteracted by the rigid branch points.<sup>42</sup> Figure 6 in fact shows that a much weaker scaling,  $2.75/M_n$ , correctly reduces the  $T_g$  data for the 11-arm star samples, underscoring the strong influence of the branch point in counteracting changes in the bulk  $T_g$  produced by chain architecture.

To evaluate how changes in bulk properties influence surface tension for some of these star polymers, PVT data were obtained for two 4-arm, and one 11-arm star PS, and representative linear PS molecules. Parts a–c of Figure 7 provide a summary of the raw data for the stars. Gross comparison of these figures indicate that PS architecture only has a small effect on the shape of the  $V$ – $T$  profiles at any given pressure. A more detailed analysis can be performed by first fitting the measured PVT data to the FOV equation-of-state.<sup>4</sup> These fits can be used to compute the CED for the respective polymers, and from it, to calculate the surface tension.<sup>27,28</sup> The measured and calculated (from PVT) surface tensions for linear and star-PS samples are provided in Figure 8. Refinements that have been included in the PVT/CED analysis consider the slight offset in the scaling curves due to conformational entropy of chains confined at narrow interfaces, particularly for high molar mass, large radii of gyration

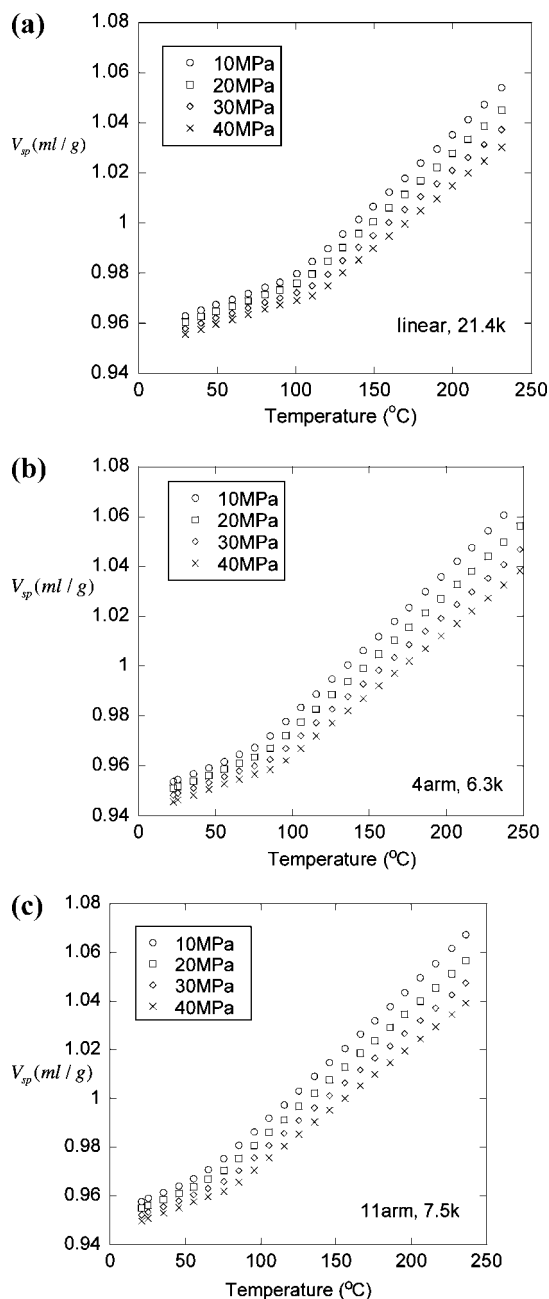


**Figure 7.** Pressure–volume–temperature data: (a) linear polystyrene,  $M_n = 21\,400$ ; (b) 4-arm star polystyrene,  $M_n = 6300$ ; (c) 11-arm star polystyrene  $M_n = 7500$ .

chains.<sup>27,28</sup> Specifically in this analysis, the 7.5K 11-arm star and the 0.7K linear PS samples were considered to be in this low  $M_n$  limit because of their very small  $R_g$ , which decreases the predictions by about 6%.<sup>28</sup> Because of the much larger radii of gyration, the 4.8K and 6.3K 4-arm stars, and the 21.4K linear molecules, these materials were considered to be in the large chain limit.

The experimental  $\gamma$  versus temperature for selected polymers in Figure 8 show that the surface entropy ( $\delta\gamma/\delta T$ ) is similar for many of the polymers in the range of molecular weight studied. This effect has never been measured before for a highly branched star. It is nonetheless consistent with the fact that the thermal expansion coefficient for these polymers and oligomers are similar. Only for very low molecular weight species do  $-\delta\gamma/\delta T$  and the thermal expansion coefficient vary from the polymer/oligomer values, and because of the high thermal expansion coefficient,  $-\delta\gamma/\delta T$  is larger for solvents.<sup>3,4,13</sup> This is seen to

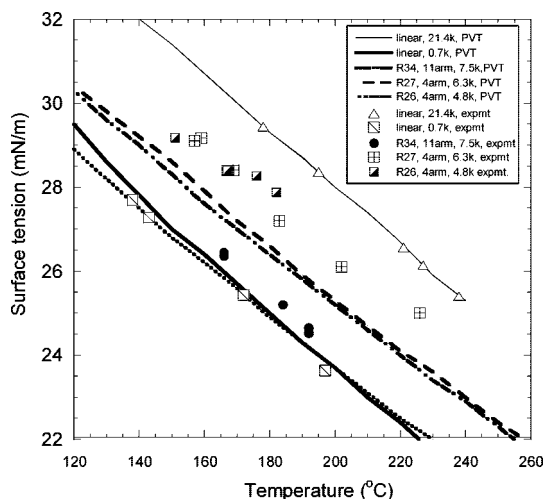


**Figure 8.** Comparison of *PVT*-based predictions with experimental surface tension data.

a small degree in the *PVT* generated curve in Figure 8, where the curve is slightly steeper for the 0.7K linear PS.

It is apparent from Figure 8 that the calculated surface tensions agree well with experiment for the two linear polymers, over the entire range of temperature studied. For all three stars, the method correctly captures the temperature-dependence of the surface-tension, but underpredicts the surface tension values. These effects are also seen for the surface tension data at 160 °C plotted in Figure 2. This figure indicates that, especially with the 4-arm stars, there is a trend toward theoretical values lower than those observed from experiment. If there was a surface activity of segments related to the *sec*-butyl containing termination, or surface excess of a low  $M_w$  fraction due to the slight polydispersity, we would expect the *PVT*-based predictions to be higher than the experimentally measured surface tension values. Here, the opposite effect is observed, indicating the lack of a substantial excess of *sec*-butyl ends. Evidentially, some elements of the physics responsible for the surface tension of the stars are not captured by the *PVT*-based analysis. Measurements using a wider range of star molecular weights are planned to explore these effects in more details.

Previous studies have shown that the surface tension of polystyrene may not be substantially modified by the presence or absence of a *sec*-butyl chain end.<sup>18</sup> Further evidence of the relative importance of end group segregation to the surface tension can be deduced from the *PVT* predicted surface tension. Our results show that the surface tension predicted from *PVT* measurements on the stars are generally lower than the experimentally measured values (Figures 2 and 8). This finding suggests that the end-group surface enrichment of *sec* butyl groups reported by Elman et al.<sup>15</sup> does not have as significant an effect on the surface tension as do bulk thermodynamic property changes due to the star architecture and end groups, at least for our system. In closing we also note that Jalbert et al.<sup>16</sup> also performed incompressible lattice simulations for polymer chains with heterogeneous end segments and compared their simulation results with experimentally measured surface tension of end-functionalized PDMS. These authors found that greater surface segregation of end groups with more surface energy difference ( $\chi_s$ ) between the end and middle segments. However, if  $\chi_s$  is not too large, the effect on the molecular weight dependence on surface tension is also small.

## Conclusions

We present the measurements of surface tension for symmetric star polymer melts with variable number of arms and

molecular weights. We find that molecular architecture plays a very important role in determining the surface tension of polymers. Specifically, for 11-arm symmetric star polystyrenes the melt surface tension is about 15% lower than linear chains at molecular weights around 7 kg/mol. Using results from a variable density lattice model that considers the effects of finite compressibility and density gradients,<sup>10,11</sup> a simple response theory is used to explain the influence of entropic and enthalpic contributions of chain ends on the surface tension of stars. This analysis indicates that both contributions are responsible for the lower surface tensions observed in PS stars. It also suggests that even without chain end functionalization, substantial reductions in a polymer's surface tension can be achieved through changes in its architecture.

We also use *PVT* measurements to characterize the effect of polymer architecture on bulk thermodynamic properties. This latter approach, while applicable to all values of  $M_n$ , appends an entropic contribution due to conformational constraints that is only applicable in the limit of large  $M_n$ .<sup>5</sup> A solution to this problem is to set this contribution to zero for small radius of gyration chains.<sup>27</sup> These measurements also show that polymer architecture can affect surface tension through its influence on the bulk thermodynamic properties, mainly due to the reduced melt density and CED with increasing numbers of chain ends. A comparison of the measured and calculated (from the CED) surface tension values suggests that chemical heterogeneity due to the *sec*-butyl terminal groups has an effect on melt surface tension that is at best of comparable magnitude to that of the chain end entropy.

**Acknowledgment.** We are grateful to the National Science Foundation (Grants DMR0551185 and DMR 0404278) for supporting this study. We thank William Kampert of DuPont for performing the DSC experiments.

## References and Notes

- (1) Defay, R.; Prigogine, I.; Bellemans, A.; Everett, D. H. *Surface Tension and Adsorption*; Longmans, Green & Co. Ltd., London, 1966.
- (2) Hong, K. M.; Noolandi, J. *Macromolecules* **1981**, *14*, 1129.
- (3) Poser, C. I.; Sanchez, I. C. *J. Colloid Interface Sci.* **1979**, *69*, 539.
- (4) Dee, G. T.; Sauer, B. B. *J. Colloid Interface Sci.* **1992**, *152*, 85.
- (5) Rabin, Y. *J. Polym. Sci., Polym. Ed.* **1984**, *22*, 335.
- (6) Theodorou, D. N. *Macromolecules* **1988**, *21*, 1400.
- (7) Hariharan, A.; Kumar, S. K.; Russel, T. P. *Macromolecules* **1990**, *23*, 3584.
- (8) Wu, D. T.; Fredrickson, G. H. *Macromolecules* **1996**, *29*, 7919.
- (9) Minnikanti, V. S.; Archer, L. A. *J. Chem. Phys.* **2005**, *122*, 084904.
- (10) Minnikanti, V. S.; Archer, L. A. *J. Chem. Phys.* **2005**, *123*, 144902.
- (11) Minnikanti, V. S.; Archer, L. A. *Macromolecules* **2006**, *39*, 7718.
- (12) Sauer, B. B.; Dee, G. T. *Macromolecules* **1991**, *24*, 2124.
- (13) Wu, S. *Polymer Interface and Adhesion*; Dekker: New York, 1982.
- (14) Fox, T. G.; Flory, P. J. *J. Polym. Sci.* **1954**, *14*, 315.
- (15) Elman, J. F.; Johs, B. D.; Long, T. E.; Koberstein, J. T. *Macromolecules* **1994**, *27*, 5341.
- (16) Jalbert, C.; Koberstein, J. T.; Hariharan, A.; Kumar, S. K. *Macromolecules* **1997**, *30*, 4481.
- (17) Jalbert, C.; Koberstein, J. T.; Yilgor, I.; Gallagher, P.; Krukonis, V. *Macromolecules* **1993**, *26*, 3069.
- (18) Hariharan, A.; Kumar, S. K.; Russell, T. P. *J. Chem. Phys.* **1993**, *98*, 4163.
- (19) Lee, J. S.; Quirk, R. P.; Foster, M. D. *Macromolecules* **2004**, *37*, 10199.
- (20) Lee, J. S.; Foster, M. D.; Wu, D. T. *Macromolecules* **2006**, *39*, 5113.
- (21) Walton, D. G.; Soo, P. P.; Mayes, A. M. *Macromolecules* **1997**, *30*, 6947.
- (22) Irvine, D. J.; Ruzette, A. G.; Mayes, A. M.; Griffith, L. G. *Biomacromolecules* **2001**, *2*, 545.
- (23) Walton, D. G.; Mayes, A. M. *Phys. Rev. E* **1996**, *54*, 2811.
- (24) Minnikanti, V. S.; Qian, Z.; Archer, L. A. *J. Chem. Phys.* **2007**, *126*, 144905.
- (25) McLain, S. J.; Sauer, B. B.; Firment, L. E. *Macromolecules* **1996**, *29*, 8211.
- (26) Mackay, M. E.; Carmezini, G.; Sauer, B. B.; Kampert, W. G. *Langmuir* **2001**, *17*, 1708.
- (27) Dee, G. T.; Sauer, B. B. *Macromol. Symp.* **1999**, *139*, 115.

- (28) Dee, G. T.; Sauer, B. B. *Computational Studies, Nanotechnology, and Solution Thermodynamics of Polymer Systems*; Dadmun, M. D., et al., Eds.; Kluwer Academic/Plenum Publishers: New York, 2001; p 29.
- (29) Sauer, B. B.; Dee, G. T. *Macromolecules* **2002**, *35*, 7024.
- (30) Ougizawa, T.; Dee, G. T.; Walsh, D. J. *Polymer* **1989**, *30*, 1675.
- (31) Flory, P. J.; Orwoll, R. A.; Vrij, A. *J. Am. Chem. Soc.* **1964**, *86*, 3507.
- (32) Dee, G. T.; Sauer, B. B. *Polymer* **1995**, *36*, 1673.
- (33) Sauer, B. B.; DiPaolo, N. V. *J. Colloid Interface Sci.* **1991**, *144*, 527.
- (34) Reiter, G. *Phys. Rev. Lett.* **1992**, *68*, 75.
- (35) Sauer, B. B. *J. Adhes. Sci. Tech.* **1992**, *6*, 955.
- (36) Fleer, G. J.; Cohen Stuart, M. A.; Scheutjens, J. M. H. M.; Cosgrove, T.; Vincent, B. *Polymers at Interfaces*; Chapman and Hill: London, 1993.
- (37) Rubinstein, M.; Colby, R. H. *Polymer Physics*; Oxford University Press Inc.: New York, 2003.
- (38) Kumar, S. K.; Jones, R. L. *Phys. Rev. Lett.* **2001**, *87*, 179601.
- (39) Kumar, S. K.; Jones, R. L. *Adv. Colloid Interface Sci.* **2001**, *94*, 33.
- (40) Sanchez, I. C.; Lacombe, R. H. *J. Phys. Chem.* **1976**, *80*, 2352.
- (41) Sauer, B. B.; Dee, G. T. *J. Colloid Interface Sci.* **1993**, *162*, 25.
- (42) Knauss, D. M.; Al-Muallem, H. A. *J. Polym. Sci., Polym. Chem.* **2000**, *38*, 4289.
- (43) Lee, J. S.; Quirk, R. P.; Foster, M. D. *Macromolecules* **2005**, *38*, 5381.
- (44) Dee, G. T.; Sauer, B. B. To be submitted for publication, 2007.

MA8002888